



4th European conference on Crystal growth
Glasgow, 2012-06

Interaction of dislocations and point defects Influence on defect patterning

Hartmut S. Leipner

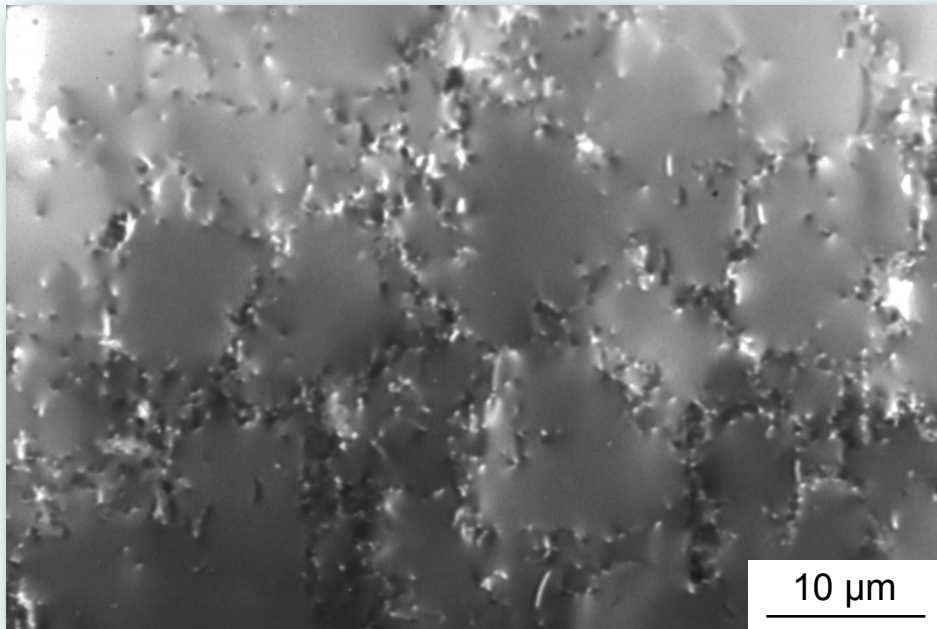


Interdisziplinäres Zentrum
für Materialwissenschaften
– Nanotechnikum Weinberg –



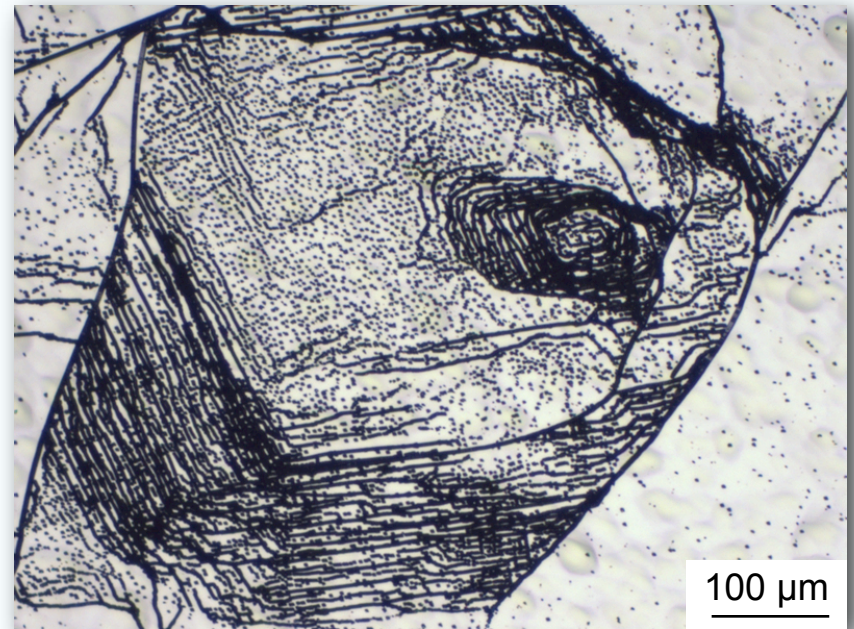
Martin-Luther-Universität Halle–Wittenberg

Dislocation patterning



Double-crystal topography of dislocation cells in LEC-grown (001) GaAs. Cu $K\alpha_1$ radiation, 511 reflection.

[W. Leitenberger]

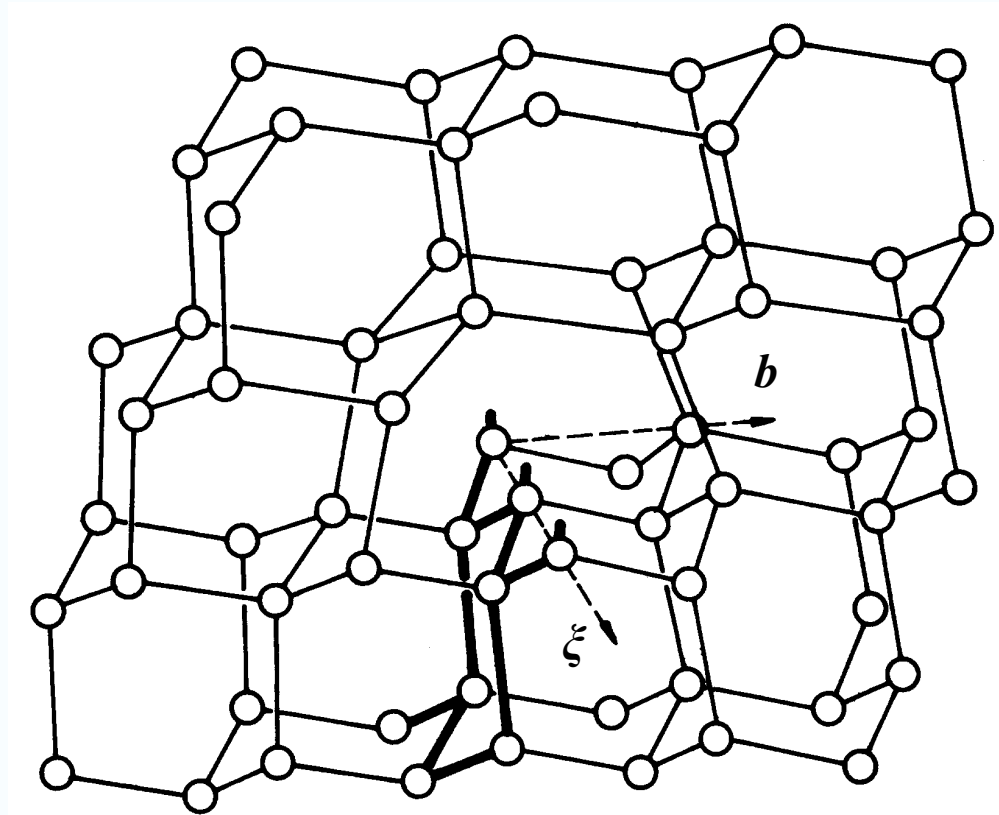


Etch-pit pattern of the dislocation distribution in multi-crystalline silicon
[D. Oriwol]

Dislocation distribution ↔ Variation in electrical/optical properties

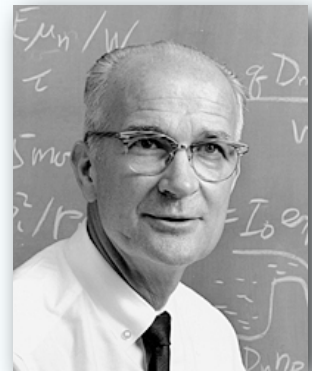
Role of intrinsic point defects and impurities

Core structure of dislocations

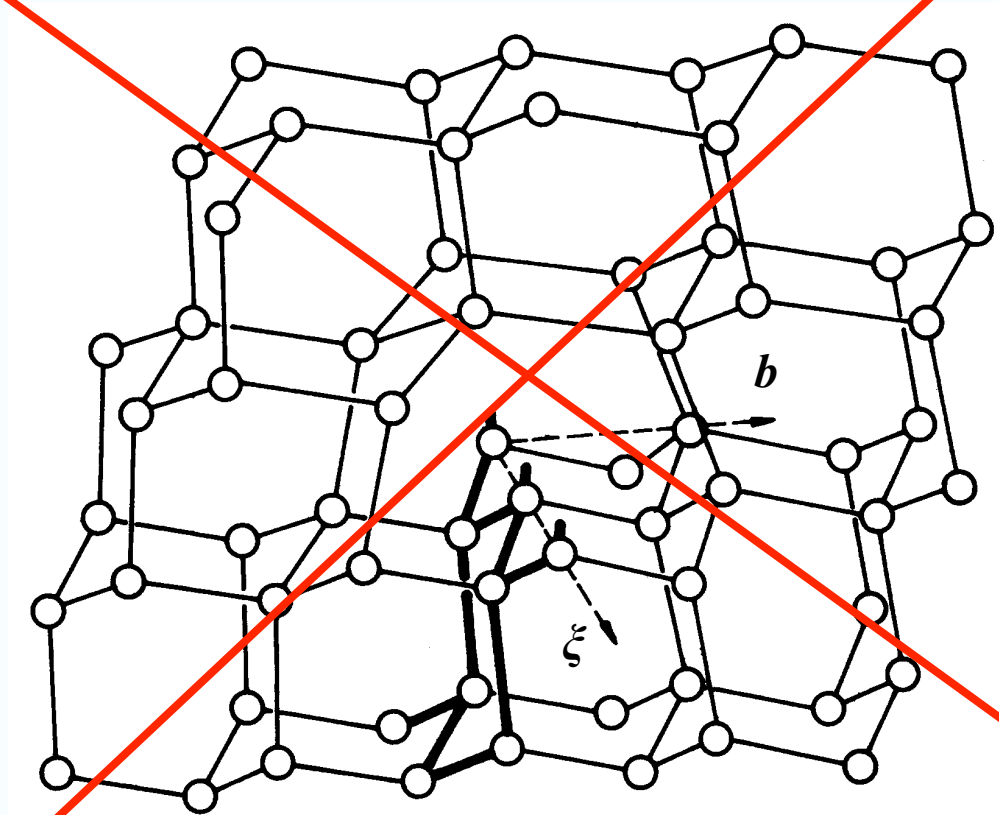


60° dislocation in the diamond structure, $b = \frac{a}{2} \langle 110 \rangle$.

[Shockley 1953]



“Ptolemaic” picture of dislocations

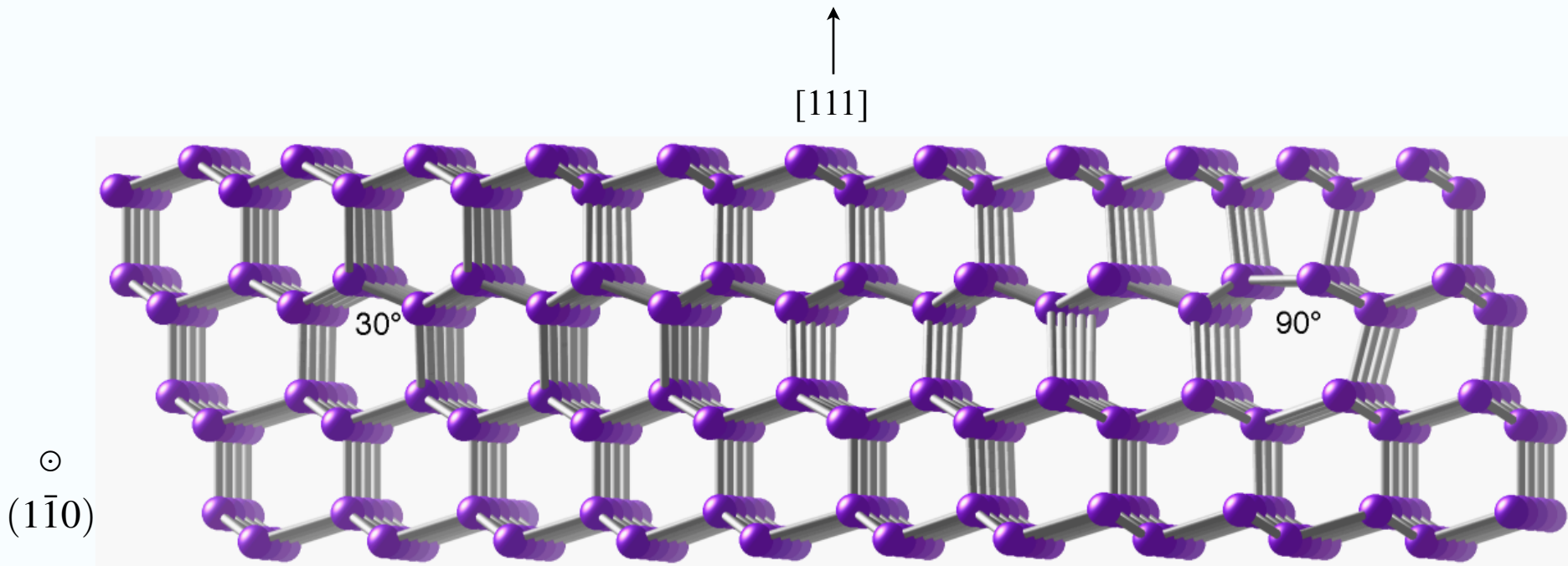


60° dislocation in the diamond structure, $\mathbf{b} = \frac{a}{2}\langle 110 \rangle$.

[Shockley 1953]



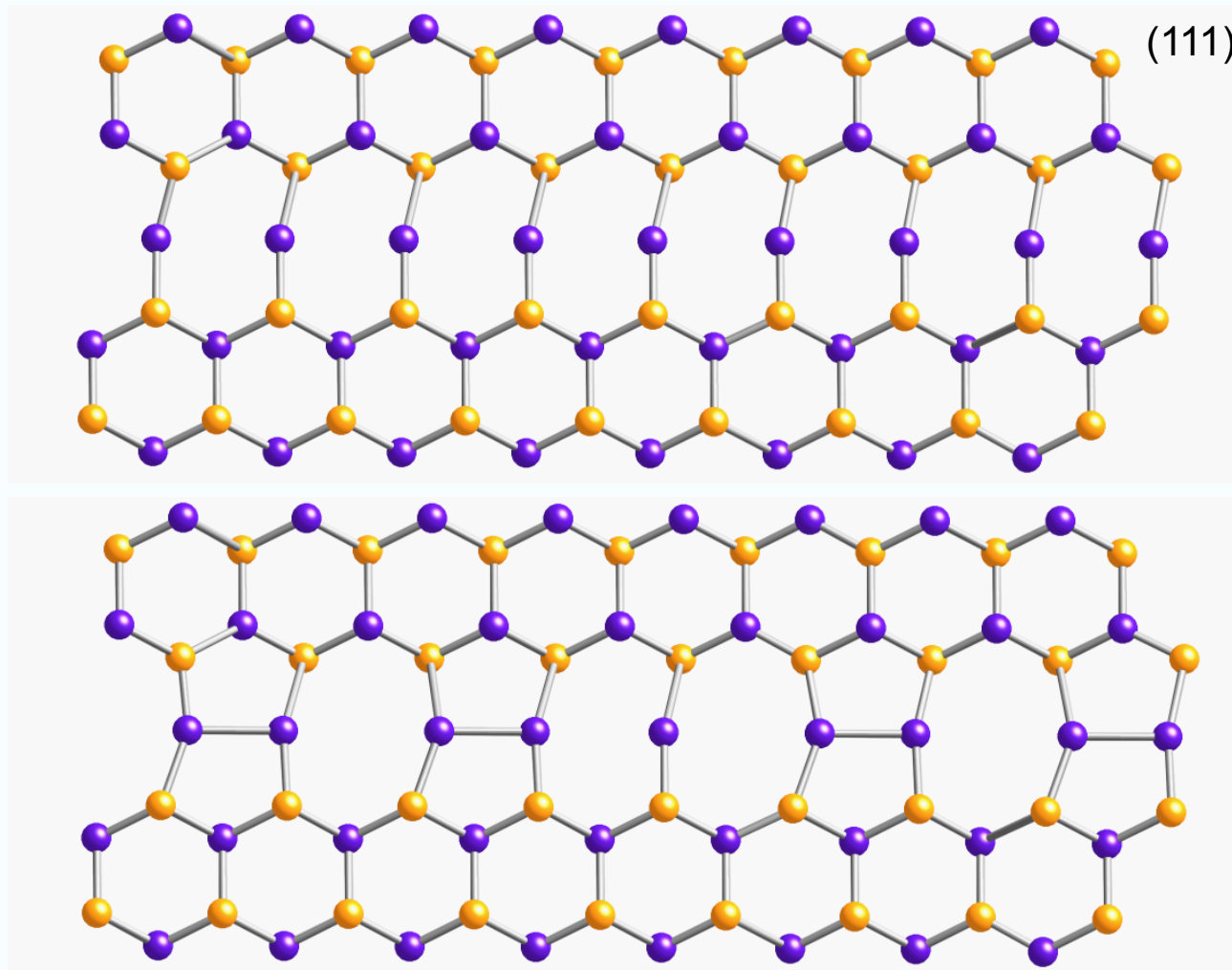
Dissociation



Dissociation of a perfect 60° dislocation in the diamond structure into a 30° and a 90° partial.

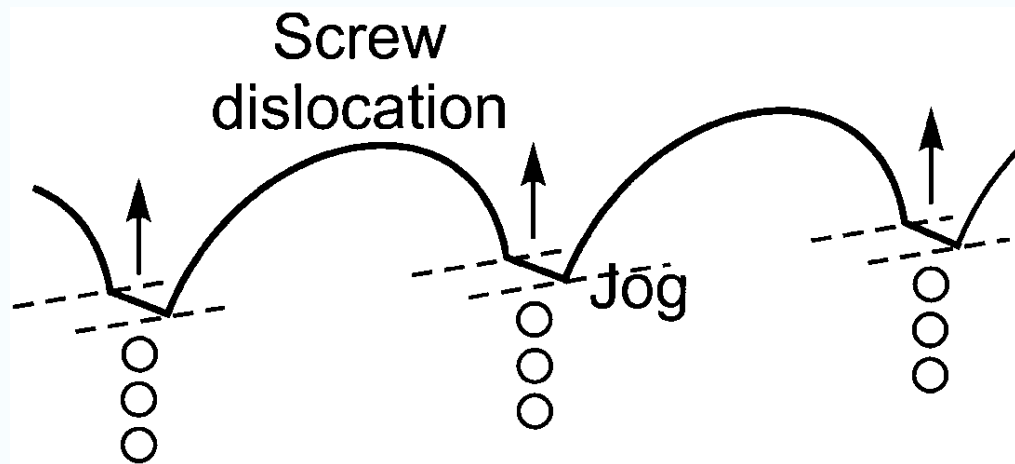
The Shockley partial dislocations, $\mathbf{b} = \frac{\mathbf{a}}{6} \langle 211 \rangle$, are separated by a stacking fault.

Reconstruction



Unreconstructed and reconstructed 30° partial

Jog dragging



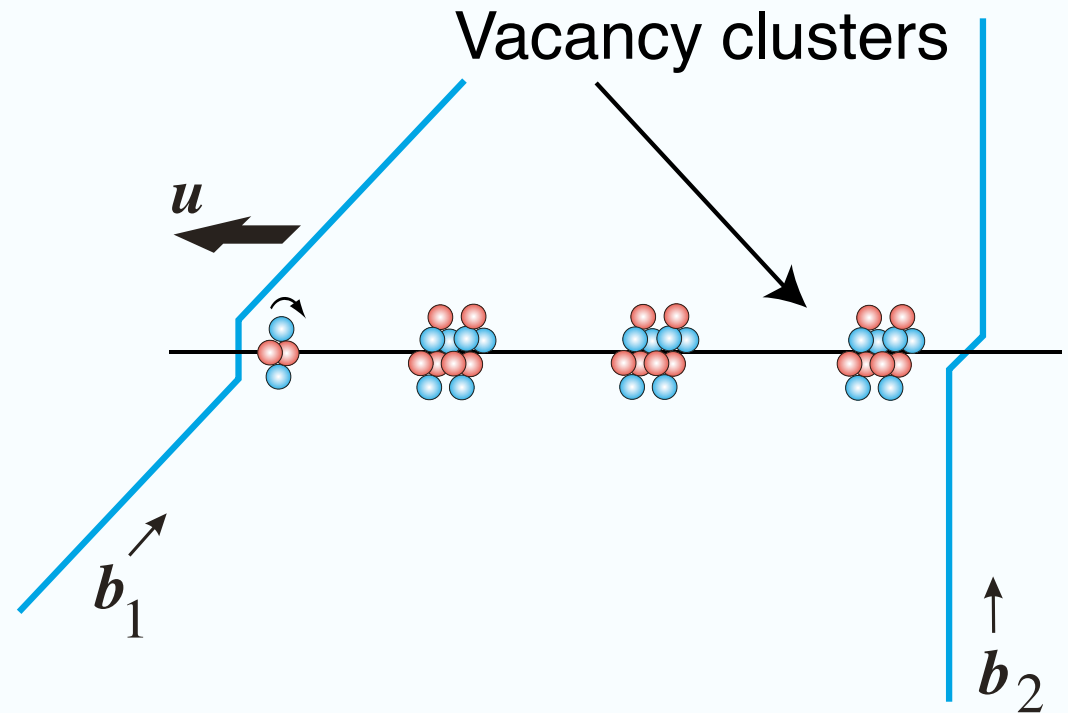
Jog dragging at screw dislocations
and point defect emission

Formation of a trail of vacancy clusters

Number of point defects

$$c = \frac{1}{\Omega} \frac{\xi_1 \cdot u \times \xi_2}{|\xi_1 \cdot u \times \xi_2|} b_1 \cdot u \times b_2$$

(per unit step
from the cutting of two screws)

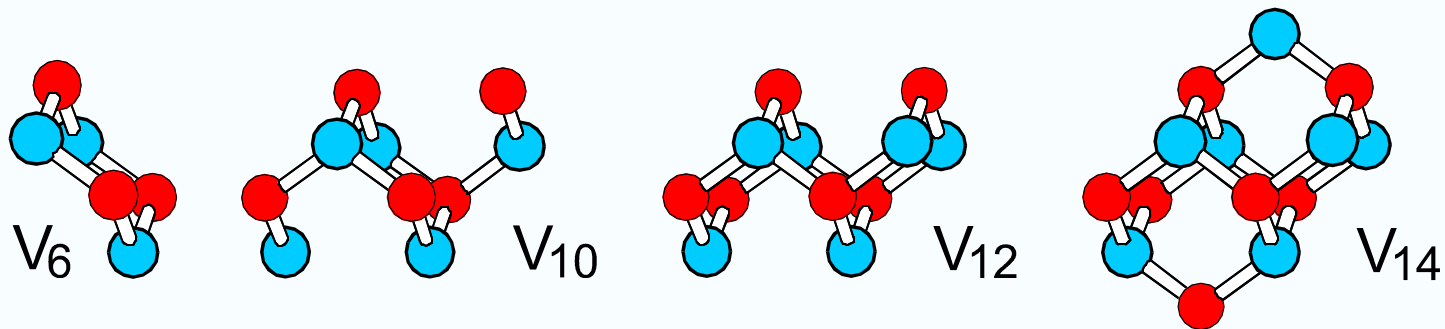


Agglomerations of vacancies as a result
of jog dragging at screw dislocations

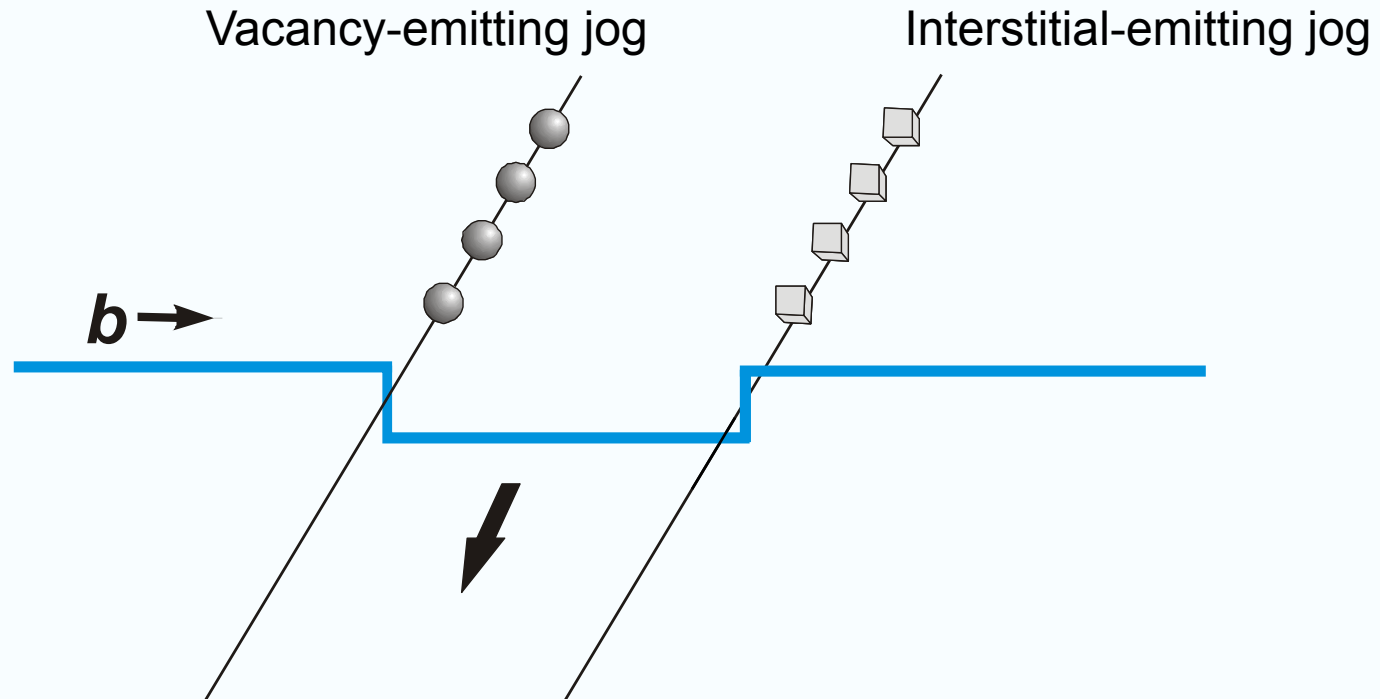
Plastic deformation

Positron annihilation measurements and density functional tight binding calculations

- ◆ Long positron lifetime due to large vacancy agglomerations
- ◆ Stable vacancy clusters V_6 , V_{10} , V_{14}
- ◆ Magic numbers of stable clusters: $n = 4i + 2, i = 1, 2, 3, \dots$

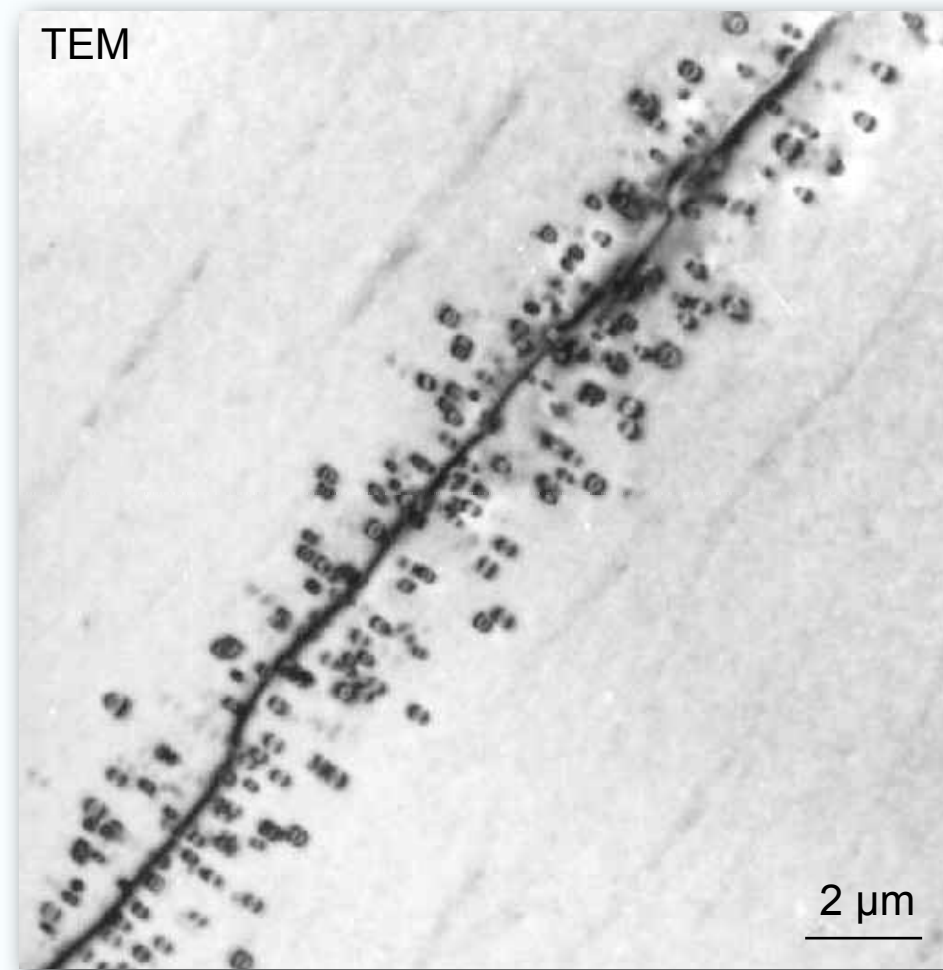


Interstitials



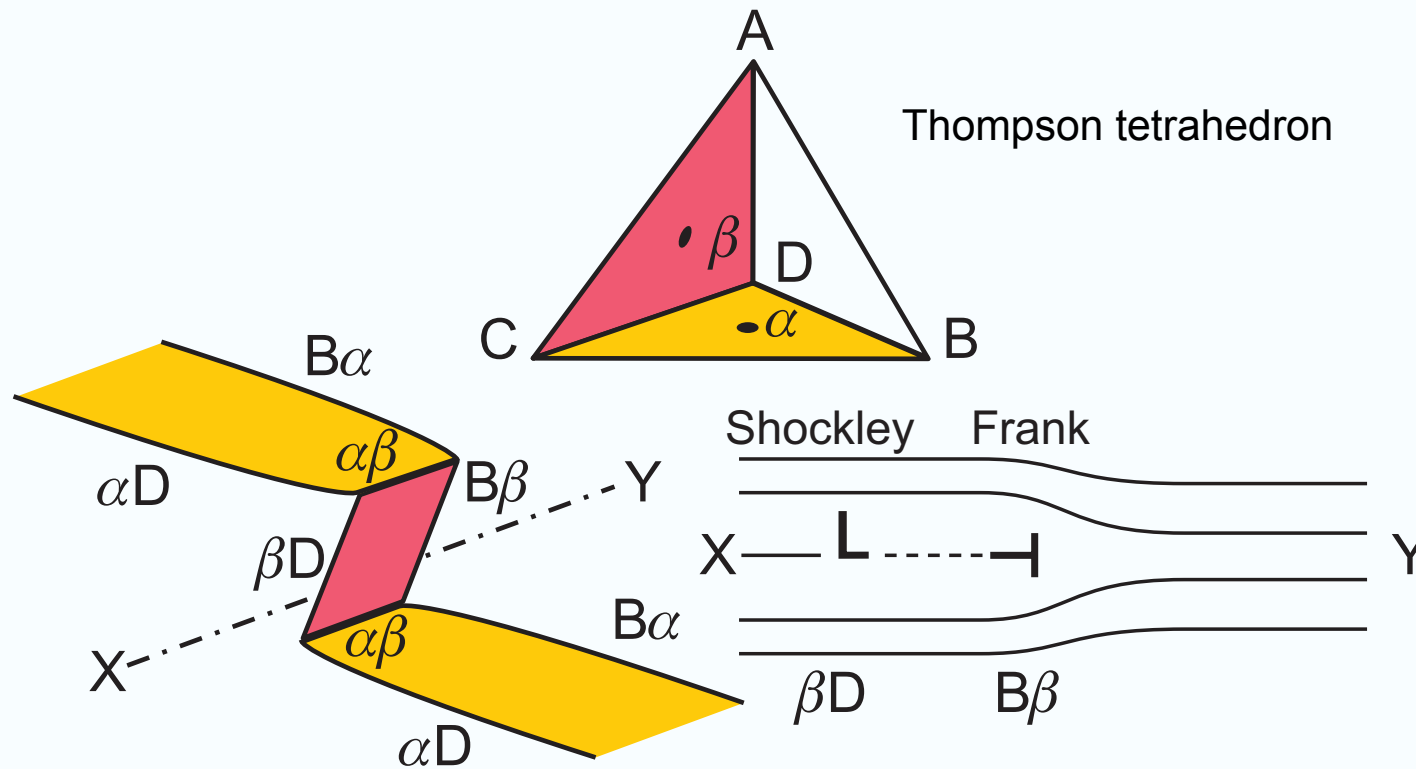
The type of the point defects emitted depends on the sign of the jog

Interstitials



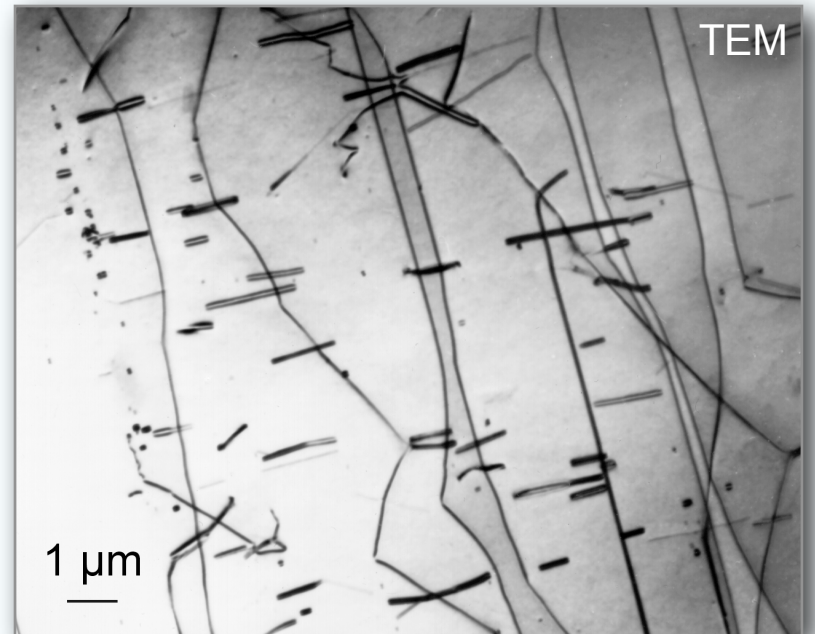
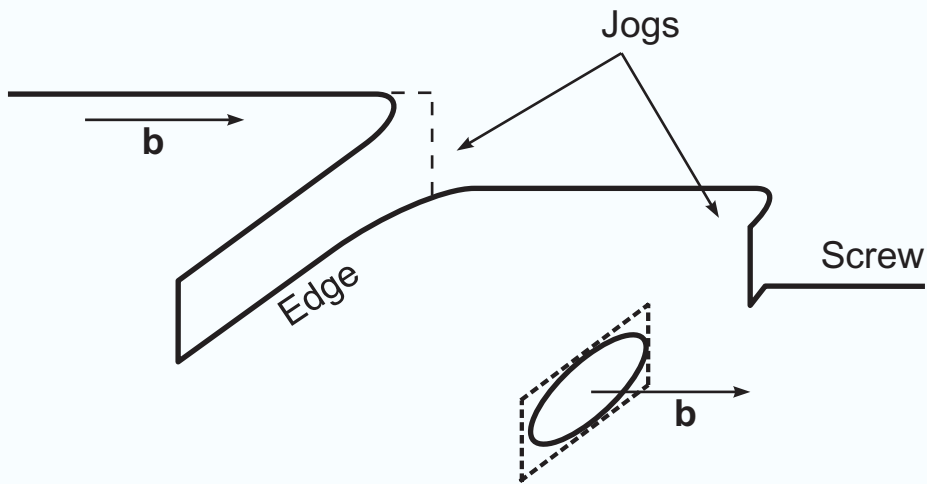
Interstitial loops surrounding a dislocation in GaAs

Extended jog



Structure of an extended jog in the acute-angle configuration on the screw **DB**. The X–Y cut illustrates the dissociation of the jog in a Shockley and a Frank partial (Burgers vectors **βD** and **Bβ**). The latter one has a pure edge character and can only follow the glide motion of the screw by the emission or absorption of point defects.

Superjogs



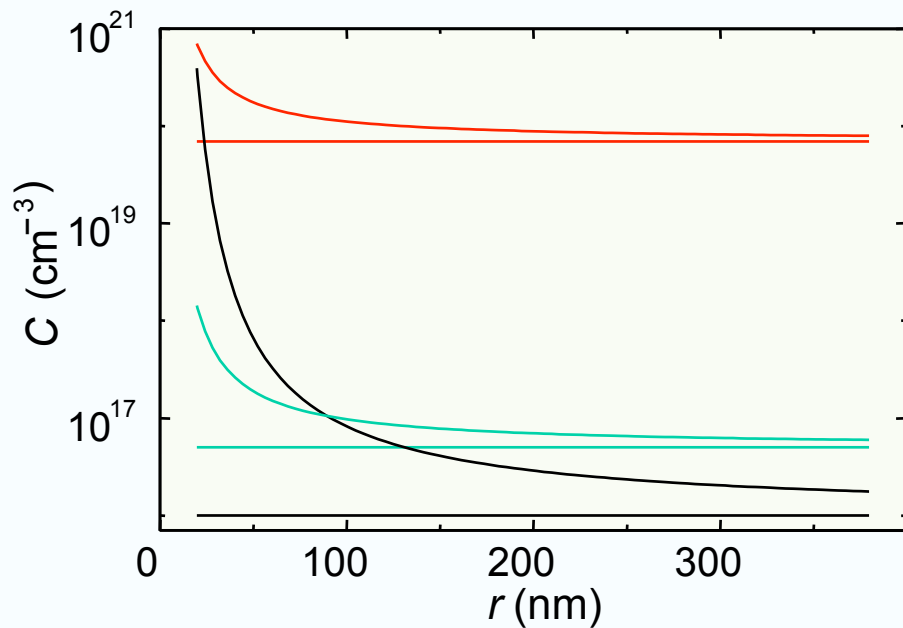
Formation of edge dipoles and prismatic dislocation loops

Cottrell atmosphere of impurities

Equilibrium case from elastic interaction

Distribution of impurities about an edge dislocation for time $t \rightarrow \infty$

$$C(r) = C_{\text{eq}} \exp\left(-\frac{\beta \sin \theta}{r k_B T}\right) \quad \beta = \frac{Gb_e}{3\pi} \frac{1+\nu}{1-\nu} \Delta V$$



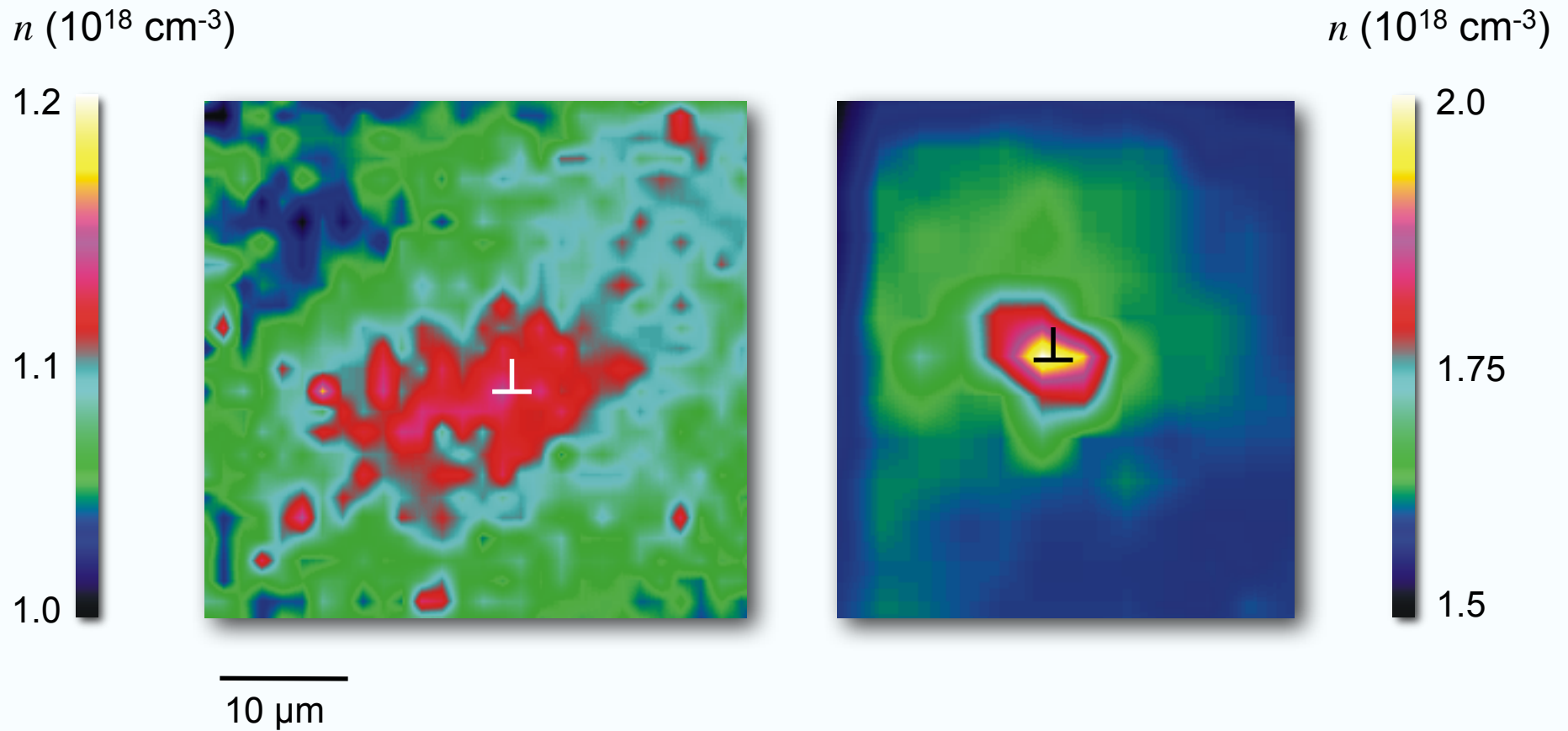
$$C_{\text{eq}} = 8 \cdot 10^{18} \text{ cm}^{-3} \text{ (1373 K)}$$

$$C_{\text{eq}} = 5 \cdot 10^{16} \text{ cm}^{-3} \text{ (973 K)}$$

$$C_{\text{eq}} = 1 \cdot 10^{16} \text{ cm}^{-3} \text{ (300 K)}$$

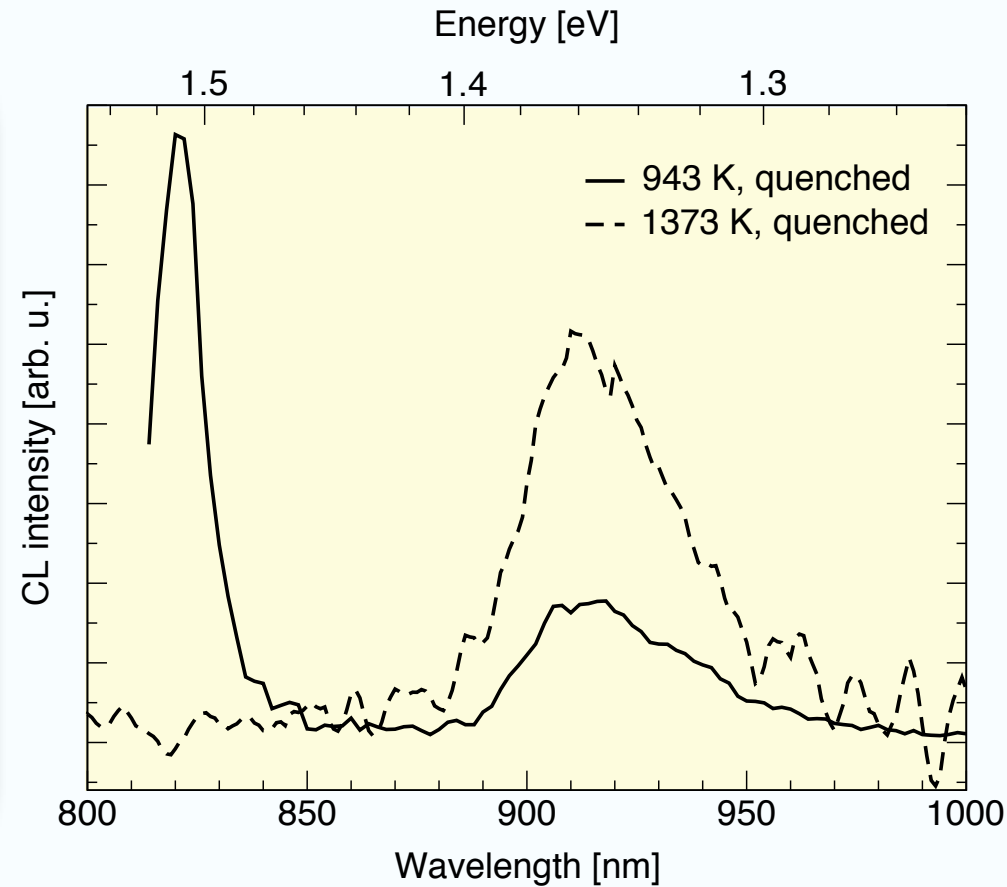
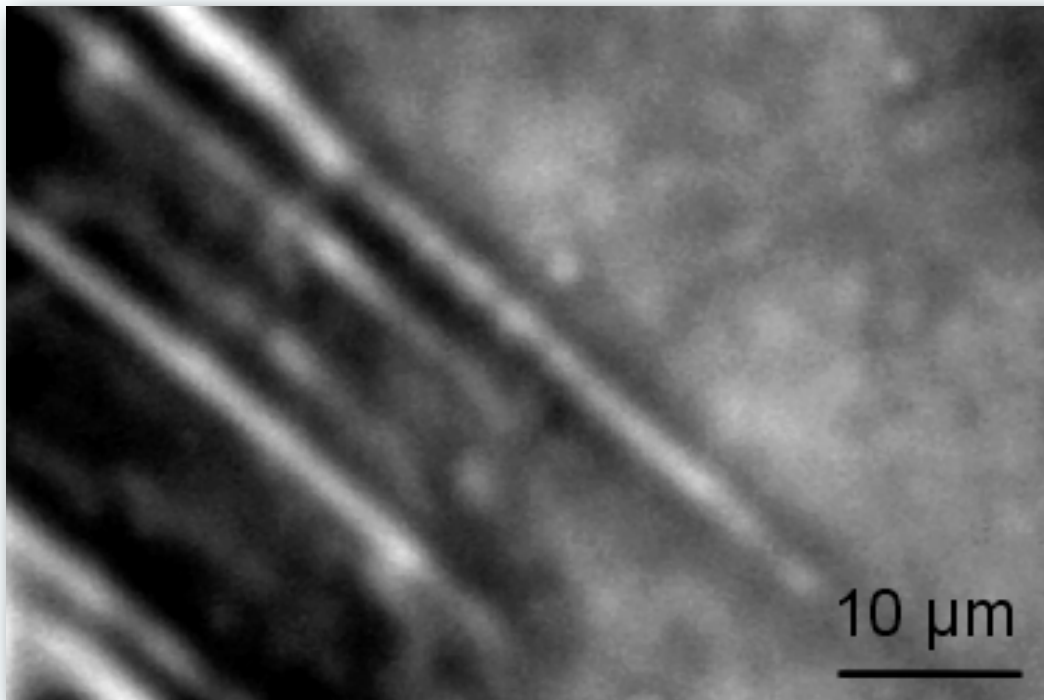
Distribution of copper at a 60° dislocation in GaAs for different solubilities C_{eq}

Distribution of charge carriers



Density of free carriers n measured by confocal Raman microscopy at dislocations in GaAs:Si (left) and GaAs:S (right)

Decorated dislocations



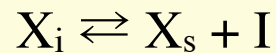
Decorated dislocations with a bright cathodoluminescence contrast in GaAs after copper in-diffusion. The bright contrast is due to the 1.36 eV emission related to Cu_{Ga} acceptors.

Microscopic processes at dislocations

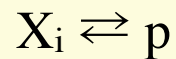
- ◆ Elastic interaction of point defects and dislocations

$$\Phi(r) = -\frac{A}{r} \sin \theta$$

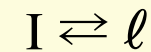
- ◆ Diffusion of point defects, e. g. via kick-out or vacancy mechanism



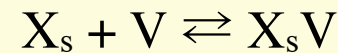
- ◆ Segregation in the core



- ◆ Formation of dislocation loops from supersaturated point defects

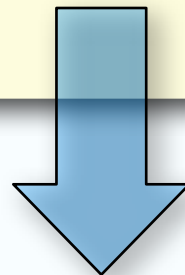


- ◆ Formation of defect complexes (intrinsic point defects/impurities)



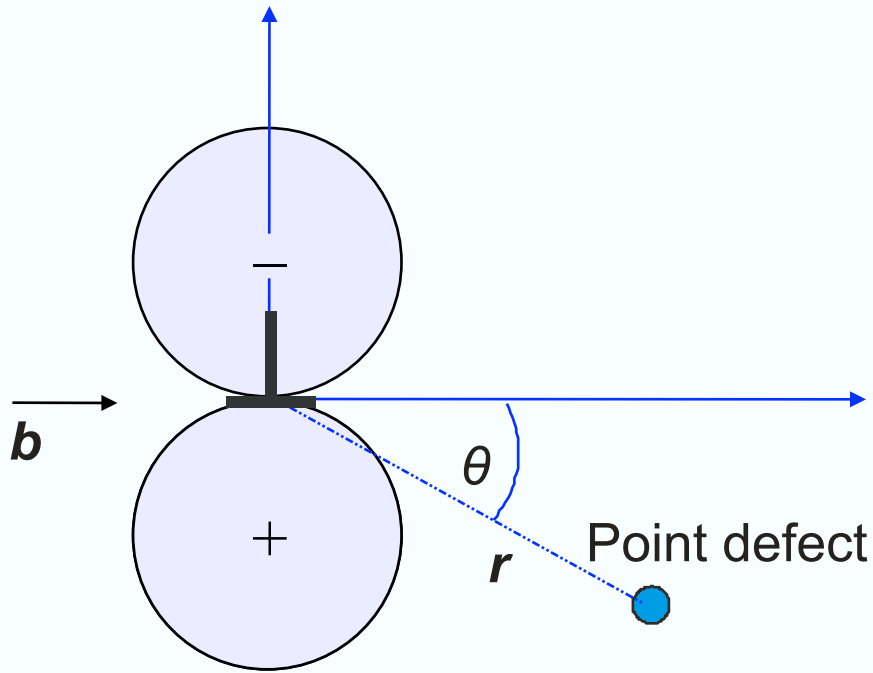
- ◆ Fermi-level effect

$$\frac{C_{X^z}}{C_{n_i}} = \left(\frac{n}{n_i} \right)^z$$



Diffusion–drift–aggregation (DDA) model

Diffusion–drift–aggregation model



Elastic interaction potential

$$\Phi(r) = -\frac{A}{r} \sin \theta \quad A = \frac{4}{3} \frac{1+\nu}{1-\nu} Grb \varepsilon$$

Drift current

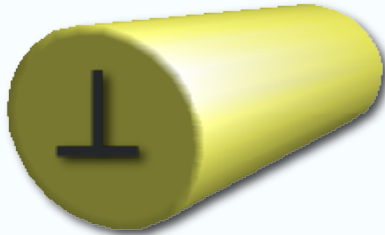
Effect of charged
point defects

Diffusion

Segregation

$$\frac{\partial C(r,t)}{\partial t} = \nabla D \left[\frac{C(r,t)}{k_B T} \nabla \Phi(r) + \nabla C(r,t) - \frac{C(r,t)}{C_{\text{eq}}(r)} \nabla C_{\text{eq}}(r) \right] - \gamma \Psi_p$$

Non-equilibrium atmosphere



- ◆ Homogeneous formation of precipitates only inside a cylinder with the radius r_0 about the dislocation core

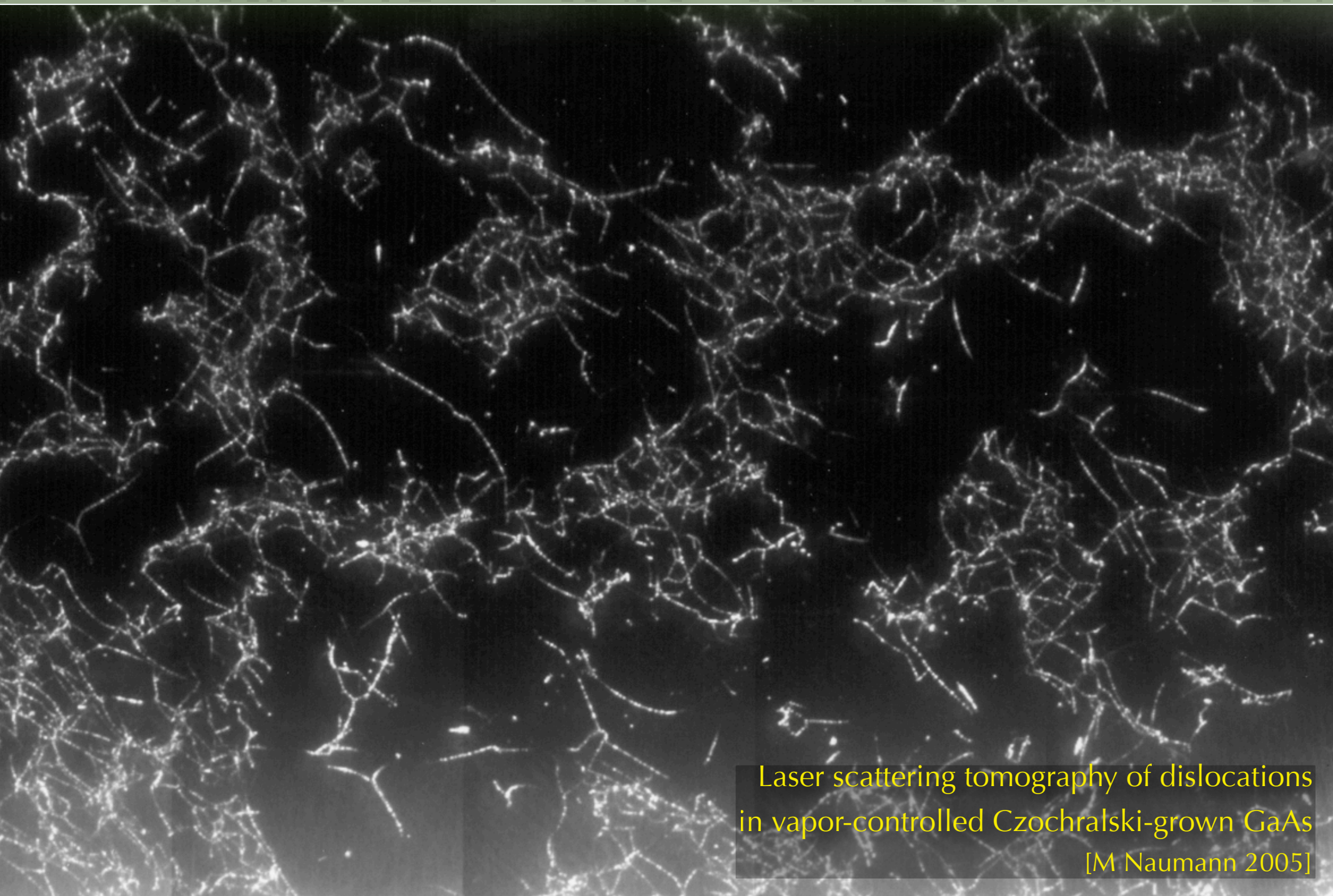
$$\gamma = \begin{cases} 1 & \text{for } r < r_0 \\ 0 & \text{for } r > r_0 \end{cases}$$

- ◆ Nucleation rate according to classical nucleation theory in the dislocation region

$$\Psi = 4\pi r_0 C(r,t)^2 D \exp\left(-\frac{16}{3} \frac{\sigma^3 V^2}{k_B T (k_B T \ln \Sigma)^2}\right)$$

(σ interface energy, V atomic volume, Σ supersaturation)

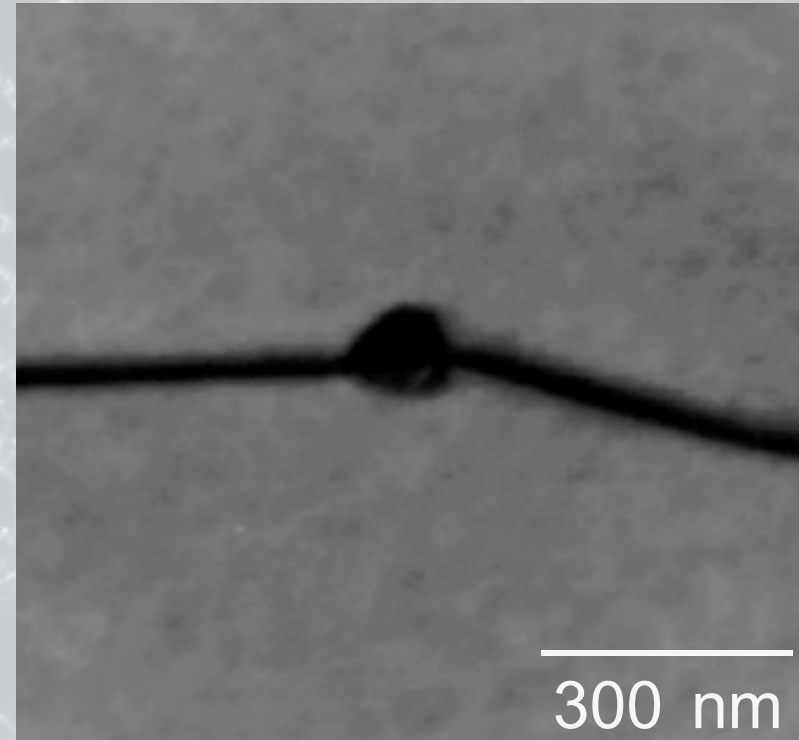
Arsenic precipitates at dislocations in GaAs



Laser scattering tomography of dislocations
in vapor-controlled Czochralski-grown GaAs
[M Naumann 2005]

Arsenic precipitates at dislocations in GaAs

- ◆ Arsenic precipitation not homogeneous along the core
- ◆ Decoration of the core?

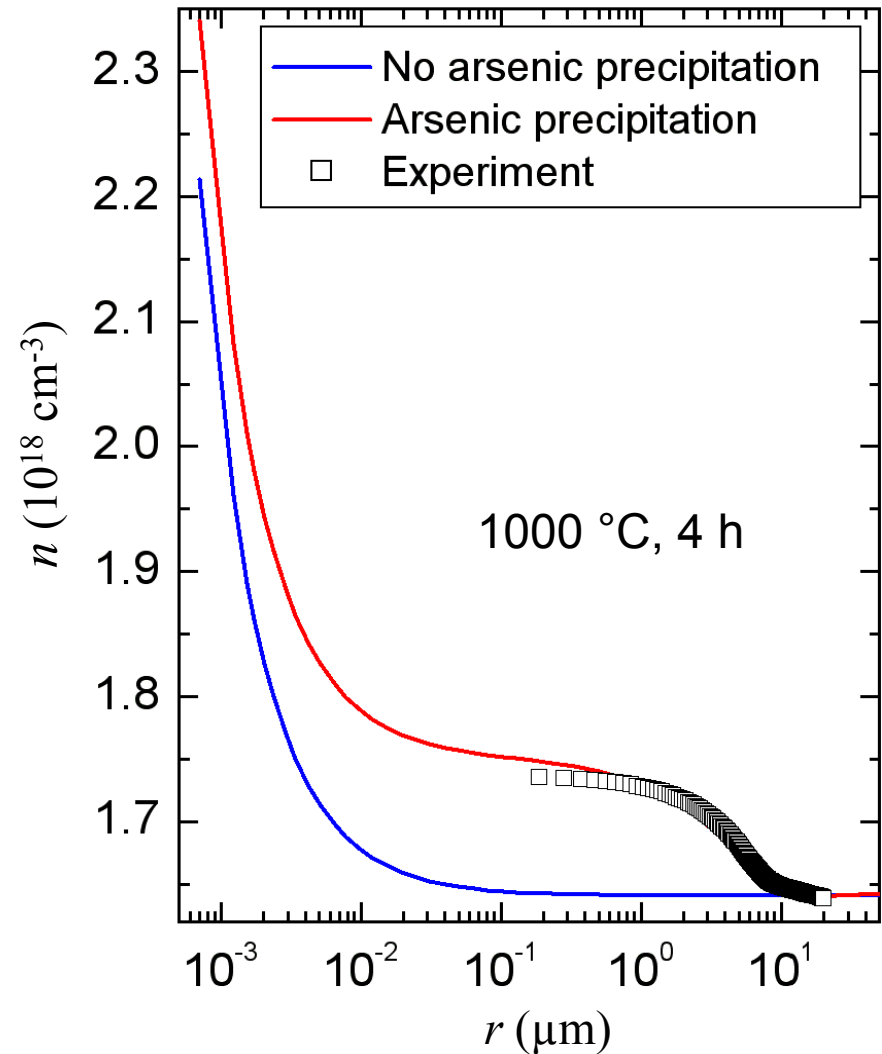


TEM bright field image of a dislocation decorated with an arsenic precipitate

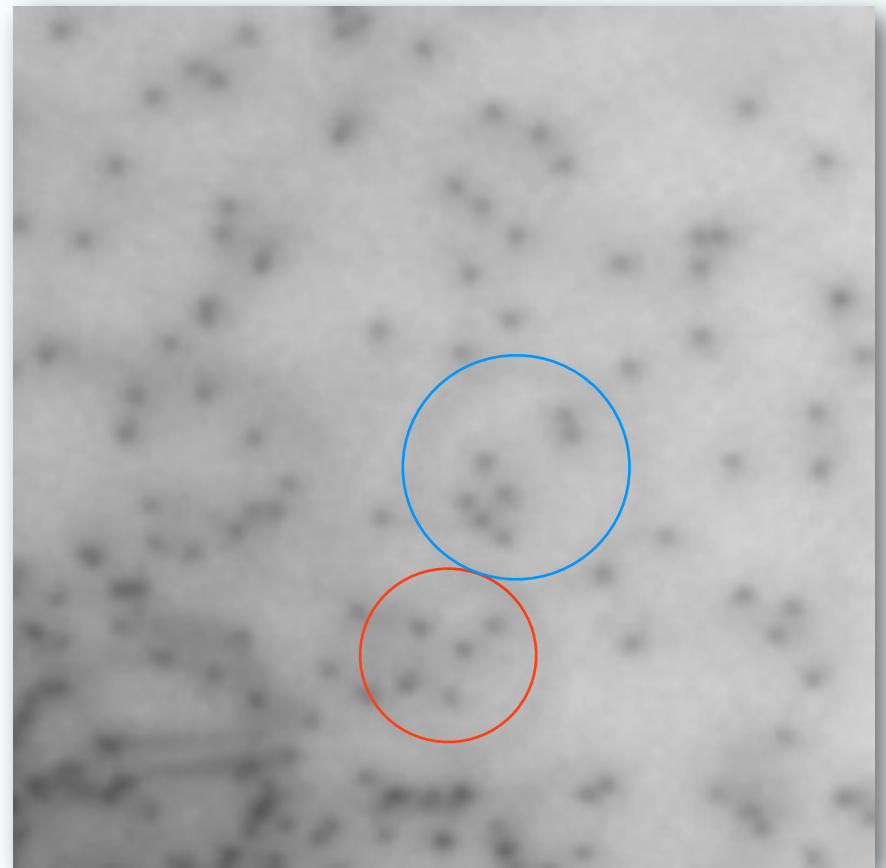
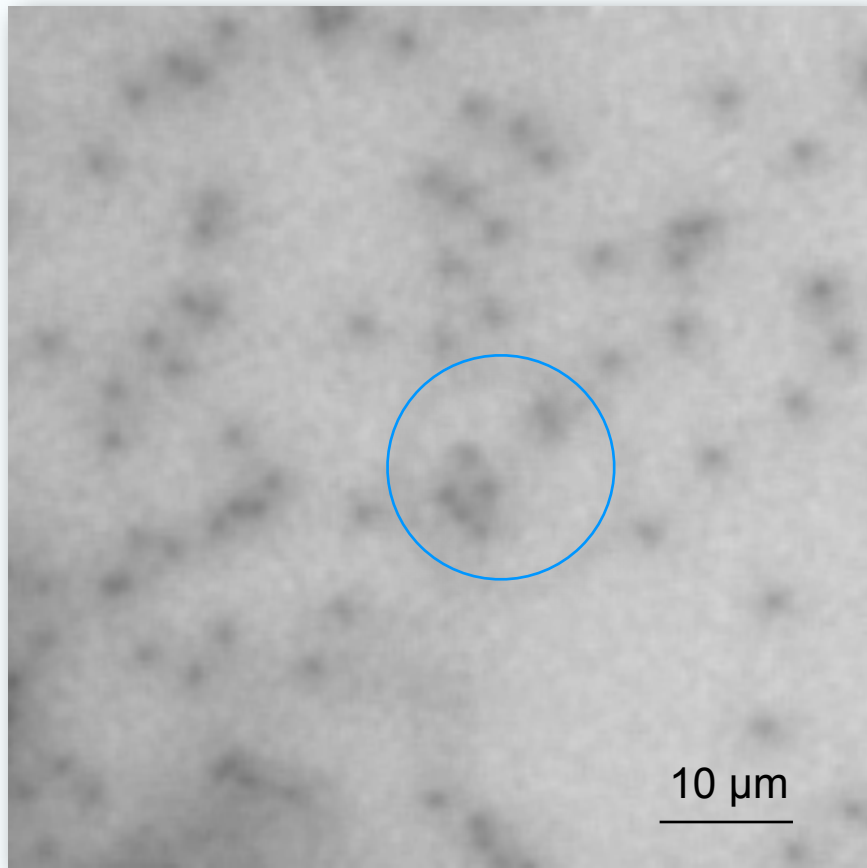
Simulation of the distribution of carriers

- ◆ From the DDA model:
variation of the concentration of defects (interstitials, charged vacancies, impurities, complexes)
- ◆ Calculation of the local carrier concentration

Distribution of free carriers
at a 60° dislocation in GaAs:S
without and with consideration of
native point defects and the
precipitation of arsenic



Cathodoluminescence of dislocations in GaN



Cathodoluminescence microscopy ($U_b = 10$ kV, $I_b \approx 15$ nA) of **in-grown** and **fresh** dislocations in gallium nitride single crystals grown by hydride vapor phase epitaxy

Cathodoluminescence of dislocations in GaN

Contrast	In-grown dislocations	Fresh dislocations
C_{\max} (%)	36 ± 1	35 ± 1
$FWHM$ (μm)	1.45 ± 0.12	1.31 ± 0.09

Cathodoluminescence microscopy ($U_b = 10$ kV, $I_b \approx 15$ nA) of **in-grown** and **fresh** dislocations in gallium nitride single crystals grown by hydride vapor phase epitaxy

Contrast similar but distinct differences in mobility

Conclusions

- ◆ Straight, perfect dislocation line hardly exists
- ◆ Complicated set of core defects;
generation of intrinsic point defects
- ◆ Hardly to separate in spectroscopic measurements different types of defects in the bulk, in the strain field of the dislocation, and in the core → local analysis necessary
- ◆ An extended defect zone, characterized by the depletion or accumulation of various point defects, is formed around dislocations.
- ◆ Electrical activity of a dislocation is the superposition of core defects, segregation of impurities in the core, accumulation/depletion of impurities in the strain field



Thanks to:

C Hübner, 雷海乐, T Staab, D Oriwol,
R Scholz, N Engler, I Ratschinski, N Wüst,
W Leitenberger, M Naumann, P Werner,
G Leibiger, F Habel, U Gösele, M Jurisch

Deutsche
Forschungsgemeinschaft

DFG



Hartmut S. Leipner



Interdisziplinäres Zentrum
für Materialwissenschaften

Martin-Luther-Universität Halle–Wittenberg

References



W Shockley Phys. Rev. **91** (1953) 228.



W T Read Phil. Mag. **45** (1954) 775.